

THE 4TH INTERNATIONAL CONFERENCE ON ALUMINUM ALLOYS

INFLUENCE OF THE DEFORMATION TEMPERATURE ON THE PARTICLE STIMULATED NUCLEATION IN THE ALLOY Al-Mn1-Mg1

O. Engler, B. Mülders, J. Hirsch*), G. Gottstein

Institut für Metallkunde und Metallphysik, RWTH Aachen, D-52056 Aachen, Germany

*) VAW aluminium AG, Research and Development, D-53014 Bonn, Germany

Abstract

During recrystallization annealing of cold rolled particle containing Al-alloys particle stimulated nucleation (PSN) occurs which gives rise to a substantial weakening of the sharpness of the typical Cube-orientation in the recrystallization textures. After deformation at elevated temperature, in contrast, a strong Cube-texture prevails, which is used in technical applications to balance the earing in the final cold rolled sheets. This change in recrystallization mechanism is examined by microstructural investigation and texture measurements in samples of the alloy Al-Mn1-Mg1 (AA3004, can body stock), which were heat-treated in such a way as to give rise to various states of precipitation prior to deformation at different temperatures.

1. Introduction

Currently, the bodies of Al-beverage cans are produced by deep drawing of sheets made in Al-Mn-Mg alloys as *e.g.* 3004. It is well known that the plastic anisotropy (earing) of Al-sheets strongly depends on their crystallographic texture. In general, the typical 45°-earing of the final gauge in a cold rolled state can be balanced by 0°/90°-earing due to a Cube-orientation {001}<100> in the texture. So, a knowledge about the mechanisms of recrystallization texture formation and in particular those affecting the Cube-texture is necessary to optimize the formability of these alloys (*e.g.* [1,2]).

During annealing of cold worked Al-Mn alloys recrystallization is accelerated by particle stimulated nucleation (PSN) within the deformation zones around the large Mn-containing particles [3-6]. In the recrystallization textures this leads to a substantial weakening of the texture sharpness at the expense of the typical Cube-texture. After deformation at elevated temperature, however, generally a strong Cube-texture prevails also in the presence of large particles [1-3,7], so that it can be assumed that PSN is less effective. The present paper gives first experimental findings of a current project on investigating the influence of deformation temperature on the recrystallization mechanisms. For that, the Al-alloy 3004 was heat-treated in order to produce various states of precipitation. The samples were subjected to deformation at ambient and at elevated temperatures. Furthermore, the influence of recovery on recrystallization was examined by intermediate recovery annealing after each cold rolling pass.

2. Experimental Methods and Characterization of the Starting Material

Samples were taken from a 25mm hot rolled plate of the alloy AA3004 (Al-1%Mn-1%Mg) prepared according to standard routes by VAW aluminium. Tensile tests were performed with different strain rates $\dot{\epsilon}$ at various temperatures. From the data $\sigma(\epsilon)$, the strain rate sensitivity index m ($= d \ln \sigma / d \ln \dot{\epsilon}$) was computed. Whereas at room temperature very low values $m \approx 0$ were obtained, m rose to 0.06 at 300°C and to 0.14 at 400°C. Thus, the temperature dependence of m is very similar to that obtained in other Al-alloys.

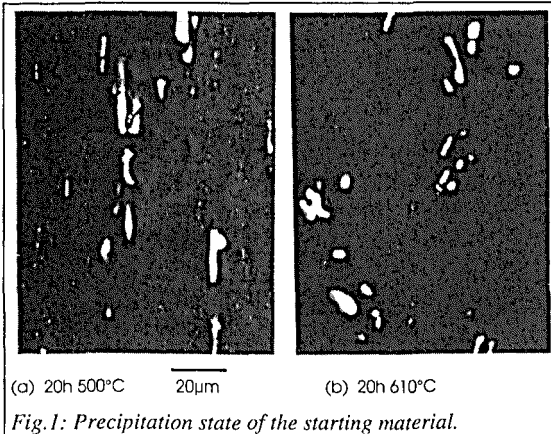


Fig.1: Precipitation state of the starting material.

The macrotexture of the plate mainly comprised the Cube-orientation with strong scatter about RD. In order to vary the precipitation state, the samples were subjected to different pre-annealing treatments. Besides characterization of the precipitation state in the SEM, the electrical conductivity σ was determined as a measure for the degree of supersaturation of solutes. In the as received hot rolled samples large constituent particles ($>10\mu\text{m}$) were present, the conductivity was $\sigma=21.5\text{m}/\Omega\text{mm}^2$. In the present paper, results of two pre-treatments will be presented:

(i) One series of samples was annealed for 20h at 500°C. This procedure led to a rather high conductivity ($\sigma=22.4\text{m}/\Omega\text{mm}^2$) which is attributed to the strong precipitation of solutes. In addition to the large constituent particles present already in the hot rolled material, a large number of smaller precipitates ($\sim 1\mu\text{m}$) were observed in this sample (Fig.1a).

(ii) During annealing for 20h at 610°C, the large constituents have slightly coagulated. The conductivity σ substantially decreased to $19.6\text{m}/\Omega\text{mm}^2$, which indicates a high amount of supersaturation caused by the re-solving of small precipitates in comparison to the initial samples (Fig.1b). The differences between the two sample sets are mainly the state of (secondary) dispersoids rather than that of the (primary) constituent particles (Fig.1).

The samples with the two different particle states were deformed according to three different routes: (i) Rolling at ambient temperature was performed by usual reversingly cold rolling in several steps to a thickness reduction of 75% (samples "CR"). (ii) In order to apply deformation at elevated temperature, samples were heated up to 375°C (within $\sim 2\text{h}$) and then immediately rolled in one step of 50% thickness reduction in a cold mill. The temperature during the rolling was measured by a thermocouple inserted in one of the samples; during the pass it rapidly dropped to $\sim 300^\circ\text{C}$. This procedure was performed two times yielding again a total reduction of 75% (samples "HR"). After this procedure, the electrical conductivity σ and, consequently, the precipitation state of the two samples was virtually unchanged.

(iii) Furthermore, the influence of recovery on the texture development was simulated by room temperature rolling followed by intermediate recovery annealings for 2min at 200°C in an oil bath between the rolling steps, *i.e.* every $\sim 10\%$ thickness reduction (samples "CR+A"). Subsequently, samples of the resulting sheets were exposed to recrystallization annealings for 30s at 425°C in a salt bath.

X-ray macrottextures were examined by computation of the ODFs from four incomplete pole figures according to the series expansion method [8]. The odd C-coefficients were derived by means of the method by Lücke *et al.* [9]. In order to avoid influences caused by a potential through thickness texture gradient, all texture measurements were performed at the centre layer of the sheets.

3. Results

3.1 Rolling Experiments

After rolling at room temperature the samples exhibited textures in which most orientations were concentrated along the so called β -fibre (Fig.2a). This orientation-fibre is typical for fcc rolling textures. It runs through the Euler angle space from the C-orientation $\{112\}\langle 111\rangle$ through S $\{123\}\langle 634\rangle$ towards the B-orientation $\{011\}\langle 211\rangle$. Besides the β -fibre rolling orientations weak occupations of the Cube orientation $\{001\}\langle 100\rangle$ were obtained (Fig.2a). In the cold rolled samples no recrystallization was observed metallographically, so the Cube-grains most probably stem from the initial (hot band) texture. For the different precipitation states, only minor differences in the textures were obtained, which will not be discussed here any further.

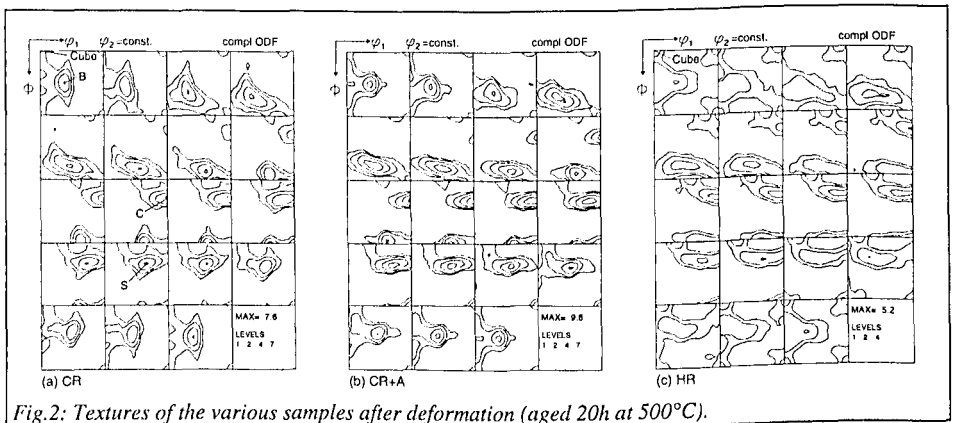


Fig.2: Textures of the various samples after deformation (aged 20h at 500°C).

In the samples which were recovery annealed between the rolling passes very similar rolling textures were found (Fig.2b). The texture intensity, however, is sharper by ~25% in contrast to the samples which were not annealed between passes. This effect of texture sharpening during recovery has already been observed and is attributed to the rearrangement of the diffuse dislocation structures into a clear subgrain structure (*cf.* [10]).

Also in the samples hot rolled at 300°C virtually no sign for recrystallization can be observed (Fig.3). However, in comparison to the cold rolled samples "CR" and "CR+A" a stronger Cube-orientation and a weakening of the rolling- (β -fibre-) orientations was obtained (Fig.2c). So, the Cube-orientations seems to be stabilized during hot deformation. Eventually, however, the rolling texture components have recrystallized during the heating period prior to the second hot rolling pass (*cf.* Sec.2). Again, for the two precipitation states no significant differences were observed.

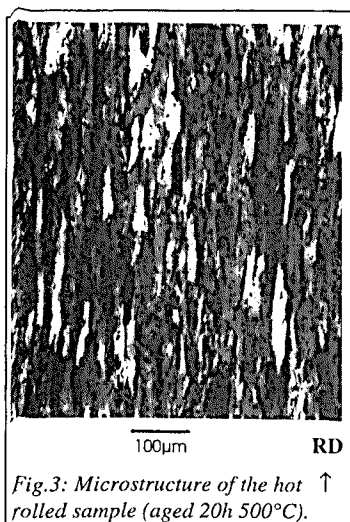


Fig.3: Microstructure of the hot rolled sample (aged 20h 500°C). ↑

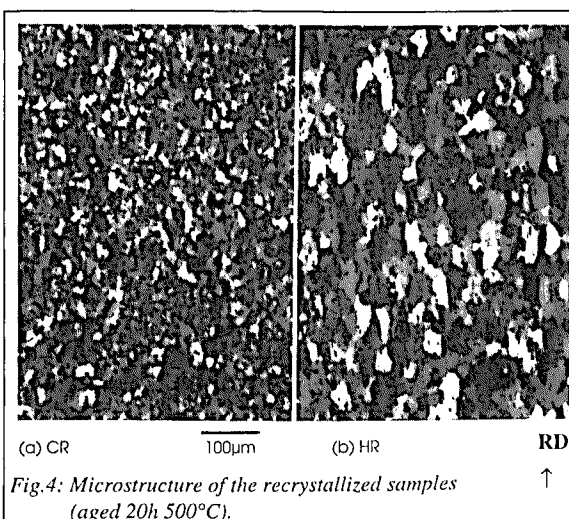


Fig.4: Microstructure of the recrystallized samples (aged 20h 500°C). ↑

3.2 Recrystallization Experiments

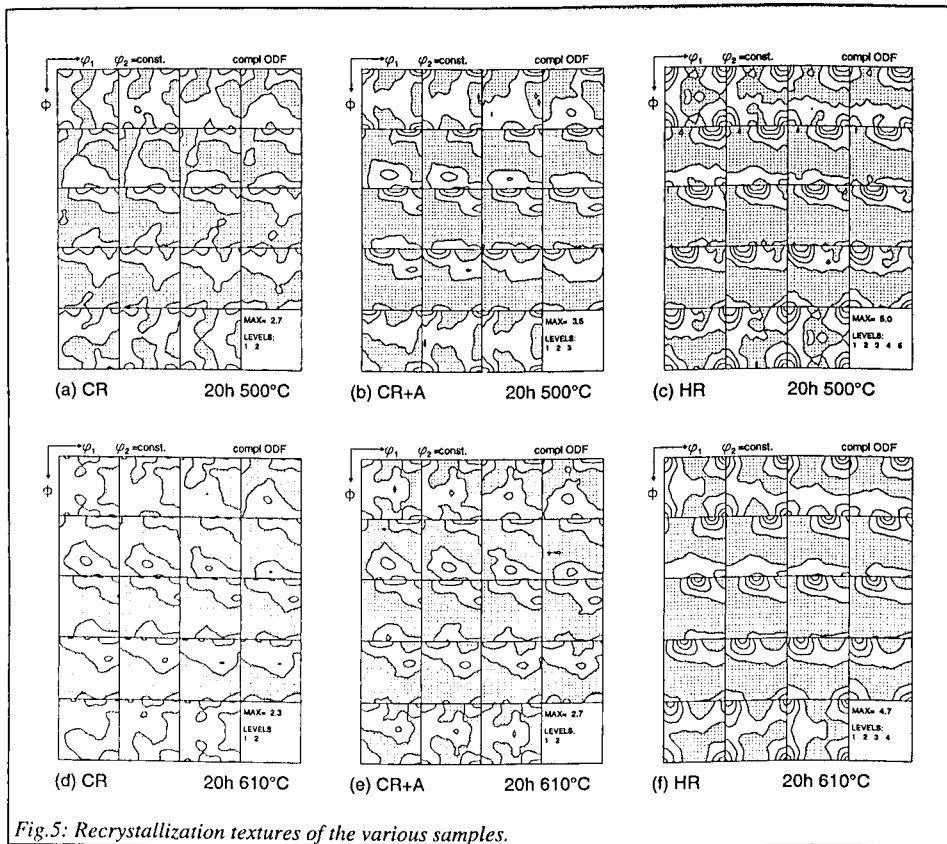
After recrystallization the samples "CR" and "CR+A" depicted very fine grained equiaxed structures ($\sim 10\mu\text{m}$, Fig.4a). In the hot rolled samples "HR" the grains were much larger after recrystallization and their shape was somewhat more elongated in RD ($\sim 20\mu\text{m} \parallel \text{ND}$; Fig.4b).

In all cases, the recrystallization textures were rather weak with a large volume of randomly oriented grains (Fig.5), which is due to the quite low level of deformation (75%). The textures of the cold rolled samples "CR" comprised a weak Cube orientation with strong scatter about RD and ND ($f(g) \approx 2.5$; Fig.5a,d). Furthermore, very weak and widely scattering occupations of the P-orientation $\{011\}\langle 122 \rangle$ were observed. The samples which were recovery annealed between passes "CR+A" showed similar recrystallization textures, the intensities of the Cube-orientation, however, were slightly stronger ($f(g) \approx 3$; Fig.5b,e). After recrystallization of the hot rolled samples "HR" this tendency is further enhanced: Here, rather strong Cube-textures ($f(g) \approx 5$; Fig.5c,f) with less scattering prevail, and moreover, the occupations of the P-orientation have diminished. With regard to the various precipitation states, for all deformation routes the samples pre-annealed at 610°C exhibited weaker textures in comparison to the samples pre-annealed at 500°C . In general, with growing texture sharpness the tendency to form the exact Cube-orientation was increased at the expense of the scattered Cube- and the P-orientations.

4. Discussion

4.1 Recrystallization after Cold Deformation of Particle Containing Al-Alloys

During recrystallization annealing of Al-samples which contain large particles principally two nucleation mechanisms can be active: (i) The typical recrystallization texture of Al-alloys is the Cube-texture with its scattering about RD towards Goss $\{011\}\langle 100 \rangle$. It is generally accepted that nuclei with Cube- and particularly with RD-rotated Cube-orientation emerge from band-like structures present in the deformed microstructure (e.g. [6,7,11-13]). However, it is still under discussion whether these bands are either transition bands according to the mechanism proposed by Dillamore and Katoh or deformed grains which comprise a Cube-orientation retained from the initial texture [7,13].



During the subsequent growth of these nuclei the exact Cube-orientation prevails due to its preferred $\sim 40^\circ \langle 111 \rangle$ orientation relationship to all symmetrically equivalent components of the rolling texture [6,12]. So, the formation of the Cube-orientation must be interpreted by both of the fundamental theories of recrystallization texture formation, oriented nucleation and growth selection [14].

(ii) During recrystallization annealing of samples which contain large particles ($>1\mu\text{m}$) PSN can take place: Owing to the dislocation/particle interactions deformation zones with very fine subgrains form around the particles [15]. During the early stages of annealing, some of these potential nuclei with preferred orientations grow into the deformed matrix (micro-growth selection) [6]. Locally, the subgrain orientations in the deformation zones can be related to the operative slip systems [15]. With respect to the entire macrotexture, however, globally a more or less random distribution of nucleus orientations exists. In that case, the resulting recrystallization texture is determined by growth selection and can, in a first approximation, be simulated by a numerical $40^\circ \langle 111 \rangle$ -transformation of the corresponding rolling textures. In general, this results in weak textures comprising the P-orientation and a characteristic scatter of Cube about ND (e.g. [6,14]).

In samples where both nucleation mechanisms are active, the final recrystallization textures then emerge from a competition between the grains stemming from the two nucleation mechanisms, Cube-bands and PSN, which leads to a weakening of the Cube-texture in favour of those orientations being attributed to PSN.

4.2 Recrystallization Textures of the Cold Rolled Samples

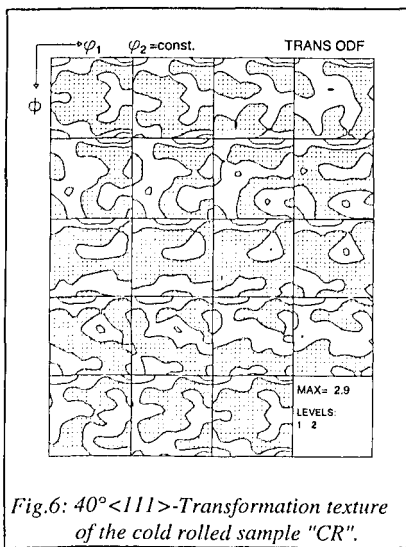


Fig.6: $40^\circ \langle 111 \rangle$ -Transformation texture of the cold rolled sample "CR".

In Fig.6 an example of the $40^\circ \langle 111 \rangle$ -transformed rolling textures of the present material is shown (cf. Fig.5). The rolling textures are still rather weak at the deformation degree of 75% (Fig.2), and therefore, the resulting transformation textures are very weak as well. But nevertheless, for the cold rolled sample aged 20h at 500°C a good agreement between the transformation textures and the recrystallization textures obtained experimentally is apparent, not only in texture sharpness but also in the position of the main components (Figs.5a,6). So it can be concluded that the precipitation state of this sample (Fig.1a) favours PSN and, therefore, the recrystallization texture is controlled by $40^\circ \langle 111 \rangle$ -growth selection out of a random spectrum of nucleus orientations.

The sample annealed for 20h at 610°C , in contrast, depicts a recrystallization texture which is even less pronounced than the transformation texture (Fig.5d). In this sample a large fraction of the alloying elements went into solution during the pre-annealing

treatment, as is indicated by the very low electrical conductivity (Sec. 2; Fig.1b). During the recrystallization anneal, the solutes which tend to precipitate are known to exert a strong influence on grain boundary motion [3,4,5]. In such case, the recrystallization texture is mainly determined by (random) nucleation rather than by subsequent growth effects [14]. The retarded growth of the nuclei also shows up in the size of recrystallized grains which was slightly smaller than in the sample being aged 20h at 500°C (Sec.3.2). However, it must be noted that during the pre-annealing at 610°C the initial grain size has coarsened and the initial texture has slightly weakened, which will also influence the final recrystallization textures.

4.3 Recrystallization Textures after Hot Deformation

In contrast to the samples "CR" rolled at room temperature, in the hot rolled samples "HR" much stronger Cube-textures form, whereas the orientations being attributed to PSN - Cube_{ND} and P - have diminished (Fig.5b,c) (cf. [1,2]). Under the assumption that the growth of the various nuclei is affected in the same way by the different rolling conditions, this result can only be explained by an enhanced efficiency of nucleation of Cube-orientation to the disadvantage of PSN. The preference of Cube-grains can be related to the dependency of both nucleation mechanisms on the deformation temperature, which means that at elevated deformation temperature (i) the formation of the Cube-orientation is favoured, and (ii) PSN becomes less effective. These two points will now be discussed:

(i) Rolling texture simulations according to Taylor type models always predict certain occupations of the Cube- and particularly of the RD-scattered Cube-orientation. In particular an increase of the strain rate sensitivity index m (Sec.2) was shown to favour the (meta)stability of Cube [16]. This means that Cube-oriented grains present in the initial texture can retain their orientation, so the band-like regions containing the Cube-orientation can survive even after high degrees of reduction [7,13] (Fig.2c). During further annealing these large Cube-oriented subgrains can easily expand into the deformed matrix. Conclusively, in comparison to samples rolled at ambient temperature, improved conditions for nucleation of the Cube-orientation are present.

(ii) PSN, in contrast, is less favourable at elevated temperature. PSN takes place in the deformation zones around the particles, if the size of the particle d_p plus the size of the deformation zone λ exceeds the critical nucleus size d_{crit} [15]:

$$2 \cdot \lambda + d_p > d_{crit} = \frac{4 \cdot \gamma_{GB}}{p_D} \quad (1)$$

(with γ_{GB} being the specific grain boundary energy of the nucleus and p_D the driving force due to the stored dislocation energy in the surrounding deformed matrix). This relation is fulfilled if the samples contain particles larger than $\sim 1\mu\text{m}$ [15].

At elevated temperature, however, the dislocation structures around the particles will be re-arranged by recovery reactions (climbing), which counteracts the formation of large misorientations around the particles and, consequently, of well-defined deformation zones [17]. According to Humphreys and Kalu [17] the critical particle size d_p necessary for forming a deformation zone depends on deformation temperature T and strain rate $\dot{\epsilon}$:

$$d_p = \left(\frac{\text{const.} \cdot \exp(-Q/kT)}{\dot{\epsilon} \cdot T} \right)^{1/3} \quad (2)$$

(with Q : activation energy for bulk diffusion). Furthermore, at elevated temperature the driving force p_D decreases (Eq. (1)) and so the critical particle size d_p necessary for the growth of the PSN-nuclei increases as well.

So, in summary, both steps of PSN, the formation of the deformation zones and the growth of nuclei out of the deformation zones, can be retarded or even completely be suppressed by dynamic recovery at high deformation temperatures and, instead, the nuclei from the Cube-bands dominate the recrystallization textures of the hot rolled samples (Fig.5c). Furthermore, the recrystallized grains in the hot rolled samples were larger and more elongated in RD compared to the cold rolled samples (Fig.4), which also indicates the reduced possibilities of PSN.

In the current study, the influence of dynamic recovery was checked by also applying an "artificial" ageing by annealing the samples for 2min at 200°C between the cold rolling passes (Sec.2). In the recrystallization textures stronger intensities of the exact Cube-orientation were obtained, whereas the Cube-ND-scatter and the P-orientation, *i.e.* the orientations being attributed to PSN, seem to be unaffected (Fig.5b). Since furthermore the recrystallized grain size was similar, it can be concluded that this recovery anneal is able to enhance only the nucleation of the Cube-grains, but does not affect PSN.

It should be noted that also in the hot rolled samples which were pre-annealed for 20h at 610°C the sharpness of the Cube-texture is reduced (*cf.* Fig.5e,f and 5b,c), although this effect is less pronounced than in the cold rolled samples. As discussed above, the supersaturation counteracts the formation of a strong recrystallization texture formed by growth selection. Furthermore, due to the larger initial grain size the number of potential Cube-nucleation sites decreases as well.

5. Conclusions

In the current investigation the influence of the deformation temperature on the recrystallization textures in the alloy 3004 was analysed. From the preliminary results, the following conclusions can be drawn:

- o The formation of the recrystallization texture can be explained by a competition between grains nucleating in Cube-bands (either transition bands or deformed grains with retained Cube-orientation) and grains originating from particle stimulated nucleation (PSN).
- o After cold rolling of samples with large particles PSN is very effective. This results in a fine grained structure and a recrystallization texture which is dominated by selected growth ($40^\circ <111>$ -transformation texture), as indicated by the Cube_{ND}- and P-orientations.
- o In samples which were supersaturated prior to deformation, precipitation during the recrystallization anneal strongly influences grain boundary movement, which gives rise to less pronounced recrystallization textures.
- o After deformation at elevated temperature, in contrast, a stronger Cube texture and larger, more elongated grains were observed. Here, the size advantage of the Cube-nuclei strongly favours Cube-oriented grains. Furthermore, PSN is suppressed as dynamic recovery counteracts the formation of viable nuclei at the particles.
- o This explanation is confirmed by the examination of samples which were recovery annealed after each pass of cold rolling. In comparison to the only cold rolled samples, stronger Cube- but similar PSN-orientations (Cube_{ND} and P) form. This indicates the beneficial influence of recovery on the Cube-nucleation sites.

Acknowledgements: The hot rolling experiments were performed with the help of Dipl.-Ing. B. Hachmann at the Institut für Bildsame Formgebung, RWTH Aachen, which is gratefully acknowledged.

References

1. W.B. Hutchinson, A. Oscarsson, Å. Karlsson, *Mat. Sci. Tech.* **5**, 1118 (1989).
2. J. Hirsch, J. Hasenclever, Proc. 3rd Int. Conf. on Al-Alloys (ICAA 3), (eds. L. Arnberg et al.), the Norwegian Inst. of Tech., Trondheim, Vol.II, 305 (1992).
3. O.S. Es-Said, J.G. Morris, in Proc. 1st Int. Conf. on Al-Alloys (ICAA 1), (eds. E.A. Starke Jr, T.H. Sanders Jr.), EMAS, 451 (1986).
4. R. Ørsund, E. Nes, *Scripta metall.* **22**, 665, 671 (1988).
5. H.E. Vatne, O. Engler, E. Nes, Proc. ICOTOM 10, *Mat. Sci. Forum* **157-162**, 1501 (1994).
6. O. Engler, P. Yang, G. Gottstein, this conference (1994)
7. O. Daaland et al., Proc. ICAA 3, as Ref. [2], Vol.II, 297 (1992).
8. H.J. Bunge, *Mathematische Methoden der Texturanalyse*, Akademie, Berlin (1969).
9. K. Lücke, J. Pospiech, J. Jura, J. Hirsch, *Z. Metallk.* **77**, 312 (1986).
10. O. Engler, I. Heckelmann, T. Rickert, J. Hirsch, K. Lücke, *Mat. Sci. Tech.* accepted (1994).
11. J. Hjelen, R. Ørsund, E. Nes, *Acta metall. mater.* **39**, 1377 (1991).
12. J. Hirsch, K. Lücke, in Proc. 7th Risø Int. Symp. (eds. N. Hansen et al.), Risø Nat. Lab., Roskilde, 361 (1986).
13. H. Weiland, J.R. Hirsch, *Textures and Microstructures* **14-18**, 647 (1991).
14. K. Lücke, O. Engler, Proc. ICAA 3, as Ref. [2], Vol.III, 439 (1992).
15. F.J. Humphreys, Proc. RECRYSTALLIZATION '90, (ed. T. Chandra), TMS, 113 (1990).
16. J. Hirsch, Proc. Hot Deformation of Al-Alloys, (eds. T.G. Langdon et al), TMS, 379 (1991).
17. F.J. Humphreys, P.N. Kalu, *Acta metall. mater.* **35**, 2815 (1987) and in Proc. 7th Risø Int. Symp., as Ref. [12], 385 (1986).